energies

MDPI

Article

Drying Characteristics, Kinetic Modeling, Energy and Exergy Analyses of Water Yam (*Dioscorea alata*) in a Hot Air Dryer

Abiodun A. Okunola [1], Timothy A. Adekanye [1], Clinton E. Okonkwo [2,*], Mohammad Kaveh [3], Mariusz Szymanek [4,*], Endurance O. Idahosa [1], Adeniyi T. Olayanju [1] and Krystyna Wojciechowska [5]

[1] Department of Agricultural and Biosystems Engineering, Landmark University, Omu-Aran P.m.b. 1001, Kwara State, Nigeria
[2] Department of Food Science, College of Food and Agriculture, United Arab Emirates University, Al Ain 15551, United Arab Emirates
[3] Department of Petroleum Engineering, College of Engineering, Knowledge University, Erbil 44001, Iraq
[4] Department of Agricultural, Forest and Transport Machinery, University of Life Sciences in Lublin, Głęboka 28, 20-612 Lublin, Poland
[5] Department of Strategy and Business Planning, Faculty of Management, Lublin University of Technology, Nadbystrzycka 38, 20-618 Lublin, Poland
* Correspondence: 700039094@uaeu.ac.ae (C.E.O.); mariusz.szymanek@up.lublin.pl (M.S.)

Abstract: In this study, drying characteristics, kinetic modelling, energy and exergy analyses of a convective hot air dryer are presented for water yam. The drying experiments were carried out at temperature levels of 50, 60, and 70 °C and slice thicknesses of 3, 6, and 9 mm. The effects of drying variables on the drying rate (DR), moisture diffusivity (D_{eff}), activation energy (E_a), energy utilization (EU), energy utilization ratio (EUR), exergy loss (EX_L), exergy efficiency (EX_{eff}), improvement potential (IP), and exergetic sustainability index (ESI) were investigated. The results showed that increasing air temperature increased the DR, D_{eff}, EU, EUR, EX_L, EX_{eff}, IP, and ESI, while increasing the slice thickness increased D_{eff} and E_a, but decreased the DR. The highest D_{eff} and E_a values were 4.2×10^{-8} m^2/s, and 53 KJ/mol, respectively. EU and EUR varied from 10 to 150 J/s and 0.39 to 0.79, respectively. EX_L and EX_{eff} varied between 2 and 12.5 J/s and 58 to 75%, respectively. Midilli's model had the best performance in predicting the moisture ratio of water yam with coefficient of determination (R^2 = 0.9998), root mean square error (RMSE = 0.0049), and sum of square error (SSE = 0.0023).

Keywords: exergy efficiency; exergy sustainability index; water yam; drying rate; exergy loss

Citation: Okunola, A.A.; Adekanye, T.A.; Okonkwo, C.E.; Kaveh, M.; Szymanek, M.; Idahosa, E.O.; Olayanju, A.T.; Wojciechowska, K. Drying Characteristics, Kinetic Modeling, Energy and Exergy Analyses of Water Yam (*Dioscorea alata*) in a Hot Air Dryer. *Energies* **2023**, *16*, 1569. https://doi.org/10.3390/en16041569

Academic Editor: Antonio Lecuona

Received: 28 December 2022
Revised: 30 January 2023
Accepted: 2 February 2023
Published: 4 February 2023

1. Introduction

Tuber crops are salient drivers of food security, income creation and sustainable development in many countries, e.g., in Africa, the tropical Pacific islands, and Southeast Asia. They serve as an important source of carbohydrate, mineral, and medicinal values to the ever-growing population of the world [1,2]. Yam is a tuberous root crop, including over 600 species, of which *Dioscorea alata*, *Dioscorea cayenensis*, and *Dioscorea rotundata* has the highest economic importance [3].

Water yam (*Dioscorea alata*) is one of the edible specie of yam; it is white in colour and originated from tropical Asian countries. It is characterized with low sugar content, high water content (70–73%), high yield, high multiplication index, and better storability in relation to other yam species. The nutritional composition of water yam includes: carbohydrate (about 22%), protein (6–8%), ash (4–5%), fat (about 1%), rich in essential minerals, and B Vitamins [3,4]. Due to the high moisture content of water yam, it is therefore necessary to convert it into a form that can be storable [5]. Low water activity retards the development of microorganism which causes food spoilage [6,7].

Drying is a technological tool for food preservation and a thermodynamic process of heat and mass transfer. It involves the simultaneous transfer of heat to food for evaporation

of water and the transport of water vapor formed away from the food [8]. Drying causes moisture reduction which increases shelf life, weight and volume reduction, reduction in packaging cost, ease of storage and transportation [9–11]. Hot air drying has been predominantly used in most agro-industries. Some of its advantages include low production and operation costs, efficient surface water removal, good physicochemical, nutritional and functional properties [8,12].

Drying is a relatively slow process, it is therefore necessary to model the drying process to prevent product degradation, reduce drying time, equipment stress, energy utilization, and product yield improvement so as to strengthen industrial design and production [11,13]. Theoretical, empirical, and semi-empirical models have been successfully used in the literature for modelling the drying kinetic of food products. Theoretical models are derived from Fick's second law of diffusion, and they describe the drying kinetic and the internal mechanism of mass transfer with respect to the geometry of the product while empirical and semi-empirical models are analogues of Fick's second law and Newton's law of cooling with little modification, they describe the statistical correlation between moisture content and drying time, though they are more convenient for practical drying systems [14].

Energy consumption is one of the engineering and technological issues of drying in the industry [15]. The high energy demand of most industrial dryers causes increase in the cost of operation, making drying process exorbitant. Energy and exergy analyses of a drying process provide information on energy savings and optimum process conditions [15]. Energy analyses quantitatively explain the energy required for a system while exergy analyses qualitatively describe the useful energy utilized by the system [16,17]. Exergy is either consumed or destroyed during the drying process (i.e., irreversible) [18]. It describes the quality of energy available in the various components of the drying systems and is important in sustainable industrial drying design systems [19–21]. Additionally, exergy analyses are important in evaluating energy consumption, energy conversion efficiency, impact of energy resources utilization on the environment, and the operation cost of a drying process [15,22].

Several investigations have been carried out on the energy and exergy analysis of drying different agricultural products using different dryers. Corzo et al. [23] carried out energy and exergy analyses of coroba slices in an air dryer; and established that energy utilization, exergy loss, and exergy efficiency increased with an increase in temperature and air velocity. Icier et al. [24] explored the exergetic performance of three different drying systems used on broccoli florets of which a fluid bed dryer showed the highest exergy efficiency. Akbulut and Durmus [25] evaluated the drying of mulberry slices in a forced solar dryer and observed that the energy utilization ratio and exergy loss decreased with an increase in the air mass flow rate while exergy efficiency increased. Aghbashlo et al. [20] conducted an experiment to analyse energy and exergy of fish oil microencapsulation in a spray dryer and obtained that energy and exergy efficiency increases at high drying temperatures (140 to 180 °C). Aviara et al. [15] observed that energy efficiency, exergy loss, and exergy efficiency of cassava starch in a tray dryer increased with an increasing temperature. Darvishi et al. [26] evaluated the effect of microwave power levels and sample thickness on the energy and exergy analysis of kiwi fruit slices, and established that energy and exergy efficiencies increased with increasing microwave power and with decreasing sample thickness. In addition, the energy efficiency was higher than exergy efficiency that was in agreement in an experiment carried by Surendhar et al. [27] on the energy and exergy analysis of turmeric in a microwave. Beigi et al. [17] conducted an exergy analysis of deep bed drying for rough rice in a convective dryer and noticed that the exergy loss and improvement potential increased with temperature and air velocity. The exergy efficiency and sustainability index of the drying process and the drying chamber increased with temperature but decreased with air velocity. Liu et al. [22] carried out an analysis of energy and exergy of mushroom in a hot air impingement dryer. It was observed that energy utilization and exergy loss increased with temperature, sample thickness and air velocity. Exergy efficiency increased with temperature and air velocity but decreased with sample

thickness. Castro et al. [28] conducted the exergy analysis of a continuous-convective dryer of onion slice as a test crop. Their results showed that exergy loss increased with drying air temperature velocity, but exergy efficiency decreased with temperature and increased with air velocity. Argo and Ubaidillah [29] explored the energy and exergy analysis of cassava chips in a tray dryer and observed that energy utilization, exergy efficiency, and exergy loss increased with drying time. Energy utilization ratio, energy efficiency, and improvement potential decreased with drying time. Parhizi et al. [30] explored pennyroyal drying in a solar-hot air dryer. An increase in temperature and bed thickness increased the energy utilization ratio, exergy loss and exergy efficiency.

The summary of these studies revealed that exergy efficiency is usually lower than energy efficiency. Energy utilization, exergy inflow, exergy outflow, energy efficiency, exergy efficiency, exergy loss, and energy utilization ratio were all affected by the drying temperatures, air velocity, microwave power levels, solar radiation, and product thickness. Although similar trends of the effects of the drying parameters have been observed from the literature, different values of the energy and exergy evaluation were reported even when the same type of dryer was used. This signifies that the exergy requirement of every crop differs even when the same dryer is used, also the environmental relative humidity and temperature can also affect its requirement. Furthermore, it has been proven from the literature that exergy analysis is certainly important in optimization of industrial drying process. Hence, information regarding exergy requirement of agricultural crops is highly beneficial to industries. Moreover, there is no information regarding the energy and exergy analyses of water yam drying using hot air convective dryer in scientific literature. Therefore, the objective of present study was to comprehensively model the drying kinetic of water yam using theoretical, semi-empirical, and empirical models and to perform the energy and exergy analyses of the drying process at different temperatures and slice thicknesses.

2. Materials and Methods

2.1. Sample Preparation

Fresh water yam was purchased from a local market in Omu-Aran, Kwara state, Nigeria. The yam tubers were manually peeled and diced in rectangular cubes (50 mm × 25 mm) of varying thickness (3, 6, and 9 mm) using a stainless knife before the commencement of the drying experiment. The different slice thickness adopted was according to Ojediran et al. [8]. The initial moisture content of the water yam was 73.70 ± 0.21% wet basis, as determined according to AOAC [31] method in triplicate, oven drying at 105 °C for 24 h [32]. About 40 g of yam slice was used to calculate the moisture content.

2.2. Drying Experimentation

2.2.1. Dryer Description and Operation

Drying experiment was conducted with a laboratory hot air dryer (Figure 1). The drying chamber consists of perforated rectangular trays (380 mm × 400 mm × 30 mm) arranged horizontally, an enclosure containing two heating elements (1 kW each), a centrifugal fan that produced the drying air at velocity (0.7 m/s), and a vent for releasing the used air. The body of the dryer was lagged with fibre glass material (thickness of 30 mm) to reduce heat loss to the surrounding and also to properly house other functional units. The automatic data logger which consists of the following parts; an Arduino interfaced with a temperature sensor (DS18B20 temperature sensor, temperature range −55 to 125 °C, resolution 9 to 12 bit, power supply 3 to 5 V, current consumption 1 mA, accuracy ±0.5 °C), a humidity sensor (DHT11 humidity sensor, humidity range 20 to 90%, power supply 3.5 to 5.5 V, resolution 16 bit, accuracy ± 1%, current consumption 0.3 mA), and an LCD screen were measurement are recorded and observed at intervals. Once the temperature inside the drying environment gets to the set temperature the heating element is thermostatically triggered OFF, and ON when it gets lower than the set temperature. Two temperature and humidity sensors were used; one was set at the air exit point while the other was

set at the drying air inlet point. These values were recorded at 10 min intervals on the LCD screen of the data logger and validated occasionally with a hygrometer (PCE-310, 0–100% relative humidity, accuracy ±3%, response time 60 s, resolution 0.1%, resistance humidity sensor) during the drying experiment. During the drying experiment, the dried air supplied constantly picks up moisture emanating from the product and discharges it through the air vent, causing weight reduction until equilibrium is reached.

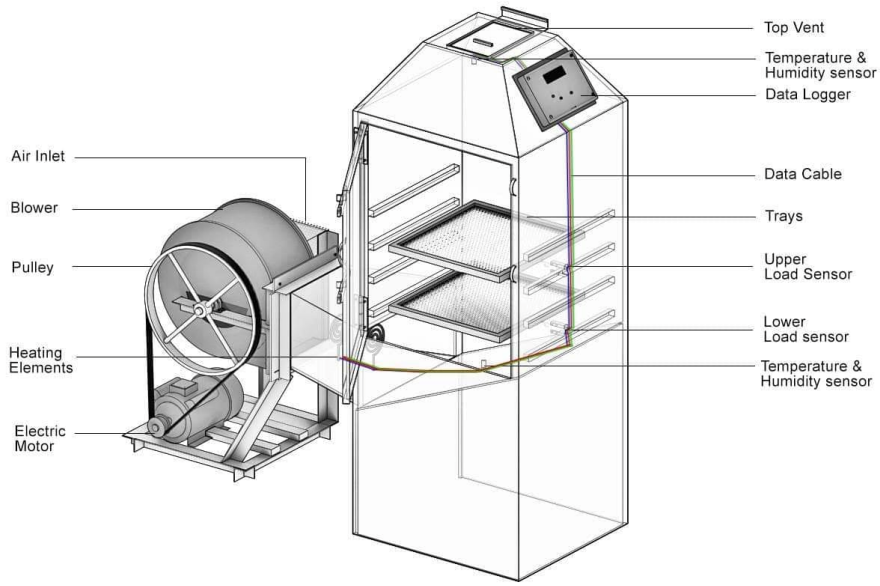

Figure 1. Schematic view of the developed laboratory hot air dryer.

2.2.2. Drying Procedure

Prior to the commencement of the drying operation, the dryer after being set to the required temperature was allowed to run for one hour for proper stabilization of the drying environment. The test procedure employed was as detailed by Aviara et al. [15] and Ojediran et al. [8]. The ambient air temperature and relative humidity varied between 27 and 32 °C and 55 and 67%, respectively during the drying period. For the experimental run, three (3) different temperatures (50, 60, and 70 °C) and slice thickness (3, 6, and 9 mm) were used, respectively. Air velocity was kept constant at (0.7 m/s). A factorial design was adopted for the combination of the variables, generating a total of nine experimental run with three replicates. Average weight loss was used for further analyses. The weight loss of the yam slice placed on the tray during drying was monitored. In the first hour, the sample was weighed at interval of 10 min, and for the next three hours it was weighed at intervals of 30 min; subsequently it was weighed at intervals of one hour until three identical readings was reached, showing the dynamic equilibrium point. The weighing balance (AND GR-200, Japan, accuracy ±0.0001 g, readability of 0.1 mg and maximum capacity 210 g) was placed very close to the dryer and weighing period of 15 s was maintained. During the course of the experiment, inlet and outlet temperature, inlet and outlet relative humidity and the ambient condition were all monitored and recorded.

2.3. Drying Kinetic

The drying kinetic for the water yam slices was computed using the following equations.

2.3.1. Moisture Content

The moisture content (MC) variation of the yam slice across the drying time was determined using Equation (1) [33]

$$M_t = \frac{W_t - W_d}{W_d} \quad (1)$$

2.3.2. Moisture Ratio

The moisture ratio (MR) was calculated from the moisture content values as shown in Equation (2) [34,35].

$$MR = \frac{M_t}{M_o} \quad (2)$$

2.3.3. Drying Rate

The drying rate reveals the moisture loss from the sample at unit time; it was calculated using Equation (3) [8,36].

$$DR = \frac{M_t - M_{t+\Delta t}}{\Delta t} \quad (3)$$

2.4. Mathematical Model

The actual data of the moisture ratio against time from the drying experiment for each treatment was fitted into ten (10) mathematical models (Table 1) using Matlab 2017a. These models were used to examine the drying kinetic of water yam in the hot air dryer. The goodness of the fit was evaluated using coefficient of determination (R^2), root mean square error (RMSE), and sum of squared errors (SSE). The best model was chosen based on the highest R^2 value, lowest RMSE, and SSE values [10,37]. These values were calculated using Equations (4)–(6).

$$R^2 = \frac{\sum(MR_{pre} - MR_{exp})^2}{\sum(MR_{AVpre} - MR_{exp})^2} \quad (4)$$

$$RMSE = \left(\frac{\sum(MR_{pre} - MR_{exp})^2}{N}\right)^{\frac{1}{2}} \quad (5)$$

$$SSE = \left[\frac{1}{N}\sum(MR_{exp} - MR_{pre})^2\right] \quad (6)$$

Table 1. Mathematical models tested for the moisture ratio of water yam.

S/N	Model Name		References
1	Page	$MR = \exp(-kt^n)$	[38]
2	Henderson and Pabis	$MR = a\exp(-kt)$	[39]
3	Newton	$MR = \exp(-kt)$	[40]
4	Aghbashlo et al.	$MR = \exp\left(-\frac{k_1 t}{1+k_2 t}\right)$	[41]
5	Logarithmic	$MR = a\exp(-kt) + c$	[42]
6	Approximation of diffusion	$MR = a\exp(-kt) + (1-a)\exp(-kbt)$	[43]
7	Two-term	$MR = a\exp(-gt) + b\exp(-ht)$	[44]
8	Wang and Singh	$MR = 1 + at + bt^2$	[45]
9	Parabolic	$MR = a + bt + ct^2$	[46]
10	Midilli et al.	$MR = \exp(-kt^n) + bt$	[47]

2.5. Moisture Diffusivity

The Fick's second law was used to describe the moisture diffusion during drying of agricultural products [14,48].

$$\frac{\partial M}{\partial t} = D_{eff}\nabla^2 M \quad (7)$$

Integrating Equation (7) for rectangular slab geometry with boundary conditions; uniform initial moisture distribution, negligible external resistance, negligible shrinkage, and constant diffusivity as given by Doymaz [45] and Srikanth et al. [2] gives Equation (8).

$$MR = \frac{M_t}{M_o} = \frac{8}{\pi^2} \sum_{n=0}^{\infty} \frac{1}{(2n+1)^2} \exp\left(-\frac{(2n+1)^2 \pi^2 D_{eff} t}{4L^2}\right) \quad (8)$$

Linearizing Equation (8) gives Equation (9)

$$\ln MR = \ln\left(\frac{8}{\pi^2}\right) - \left(\frac{\pi^2 D_{eff} t}{4L^2}\right) \quad (9)$$

A plot of ln(MR) against drying time [t] gave a curve with slope K and the moisture diffusivity can be calculated from Equation (10).

$$K = \frac{\pi^2 D_{eff}}{4L^2} \quad (10)$$

2.6. Activation Energy

Activation energy is the energy required for moisture diffusion during drying of agricultural products. The Arrhenius equation is used in describing the correlation between moisture diffusivity and activation energy [8].

$$D_{eff} = D_0 \exp\left(-\frac{E_a}{R(T + 273.15)}\right) \quad (11)$$

Linearizing Arrhenius equation

$$\ln D_{eff} = \ln D_0 - \frac{E_a}{R(T + 273.15)} \quad (12)$$

2.7. Energy Analyses

The energy analyses for the water yam drying process were calculated from the data obtained during the experiment. The flow was assumed to be steady. The first law of thermodynamics for an open system was adopted in these analyses [15,25].

Energy balance equation:

$$Q - W = \Delta U = \sum \dot{M}_{A2} \left[h_2 + \frac{{v_2}^2}{2}\right] - \sum \dot{M}_{A1} \left[h_1 + \frac{{v_1}^2}{2}\right] \quad (13)$$

Assume no mechanical work is performed, no resultant motion and equal mass flow rate at inlet at outlet during the drying process of the yam slices. Therefore, Equation (13) becomes:

$$Q = \dot{M}_A (h_2 - h_1) \quad (14)$$

The mass flow rate and air enthalpies in the dryer were calculated from Equations (15) and (16), respectively.

$$\dot{M}_A = \rho_A \dot{V}_A \quad (15)$$

$$h = C_{pA} T_{dA} + H h_{sat} \quad (16)$$

$$C_{pA} = 1.003 + 0.00005 T_{dA} \quad (17)$$

2.7.1. Energy Utilization

The energy utilization of the dryer for drying of the yam slices was calculated from Equation (18) [22].

$$EU = \dot{M}_A (h_2 - h_1) \quad (18)$$

2.7.2. Energy Utilization Ratio

Energy utilization ratio (EUR) of the drying unit was calculated using Equation (19) [15,49].

$$EUR = \frac{\dot{M}_A(h_1 - h_2)}{\dot{M}_A(h_1 - h_\infty)} \quad (19)$$

2.8. Exergy Analyses

The analyses of exergy for the drying process of the yam slices in a hot air dryer was carried out using the second law of thermodynamics which states that heat cannot flow from a body at lower temperature to a body at higher temperature spontaneously except using an external factor. The second law shows that when an amount of heat energy is supplied to a system, a part of energy becomes un-transformable to useful work while the other part would be use by the system to do work. The exergy balance is described by Equation (20) for an open system [15,25,29].

$$EX = [U - U_\infty] - T_o[S - S_\infty] + P_\infty[V - V_\infty] + \frac{v^2}{2} + [Z - Z_\infty]g + V[P - P_\infty] \quad (20)$$

There was no relative motion or vibration in the dryer. Therefore, the gravity and momentum components were dropped, Equation (20) reduced to Equation (21):

$$EX = [U + PV] - [U_\infty + P_\infty V_\infty] - T_o[S - S_\infty] \quad (21)$$

Replacing U+PV in Equation (22) with enthalpy (h) gives Equation (22):

$$EX = C_{pA}\left[(T_{dA} - T_o) - T_o \ln \frac{T_{dA}}{T_o}\right] \quad (22)$$

2.8.1. Exergy Inflow, Exergy Outflow and Exergy Loss

Exergy inflow, exergy outflow, and exergy loss were calculated using Equations (23)–(25) [37].

$$EX_1 = C_{pA1}\left[(T_{dA1} - T_o) - T_o \ln \frac{T_{dA1}}{T_o}\right] \quad (23)$$

$$EX_2 = C_{pA2}\left[(T_{dA2} - T_o) - T_o \ln \frac{T_{dA2}}{T_o}\right] \quad (24)$$

$$EX_L = EX_1 - EX_2 \quad (25)$$

2.8.2. Exergy Efficiency

The exergy efficiency of the dryer in moisture diffusion of the yam slice was calculated using Equation (26) [16,22].

$$EX_{eff} = \frac{EX_1 - EX_L}{EX_1} \times 100 \quad (26)$$

2.8.3. Improvement Potential

Exergetic improvement potential rate is also referred to the improvement potential for the dryer. Exergy improvement potential is the amount of exergy that can be reused by minimizing wasted exergy. It was calculated using Equation (27) [15,50].

$$I_P = \left(1 - \left(1 - \left(\frac{EX_L}{EX_1}\right)\right)\right) \times (EX_1 - EX_2) \quad (27)$$

2.8.4. Exergetic Sustainability Index

The exergetic sustainability index (ESI) of the drying process was evaluated using Equation (28) [17,28].

$$\mathrm{ESI} = \frac{1}{1 - \mathrm{EX_{eff}}} \tag{28}$$

The reference condition of the drying environment is T_o = 29.5 °C, relative humidity of 61%, and P_∞ of 101.3 kPa

2.9. Statistical Analyses

Microsoft Excel (version 2016) was used in analysing the experimental data, calculating the standard deviation, and plotting the graphs. MATLAB software (version R2017a) was used for fitting the drying kinetic data in the different mathematical models.

2.10. Uncertainty Analyses

Uncertainty analyses are usually performed for reliability and soundness of the experimental and predicted data obtained [14,51]. The uncertainty analysis was conducted using Equation (29).

$$\mathrm{U} = \left[\left(\frac{\partial \mathrm{y}}{\partial \mathrm{x_1}} \mathrm{u_1} \right)^2 + \left(\frac{\partial \mathrm{y}}{\partial \mathrm{x_2}} \mathrm{u_2} \right)^2 + \left(\frac{\partial \mathrm{y}}{\partial \mathrm{x_3}} \mathrm{u_3} \right)^2 + \cdots + \left(\frac{\partial \mathrm{y}}{\partial \mathrm{x_n}} \mathrm{u_n} \right)^2 \right]^{\frac{1}{2}} \tag{29}$$

3. Results

3.1. Drying Kinetic

The variation between the MR and the time for all drying parameters (temperatures versus slice thickness) is shown in Figure 2a–c. MR was found to decrease by an increase in drying time. The decrease in moisture ratio with time was faster at higher temperatures and smaller slice thicknesses. The temperature rise increases the heat and mass transfer rate. At the minimum slice thickness, there is lower volume of water and faster moisture transport from the core of the slice for evaporation [8]. The shortest drying time was observed at the maximum temperature (70 °C) and the minimum slice thickness (3 mm) by 900 min while the longest was at the minimum temperature (50 °C) and maximum slice thickness (3 mm) by 1860 min. A similar trend on the effect of temperature and slice thickness on drying kinetic has been reported by Fang et al. [33] for the effect of temperature on Chinese yam, Onwude et al. [52] for the effect of temperature on sweet potato, and Ojediran et al. [8] for the effect of temperature and slice thickness on *Dioscorea rotundata*.

3.2. Drying Rate

The effect of temperature and slice thickness on the drying rate (DR) versus moisture content is presented in Figure 3a–c. Drying rate increased with an increase in moisture content. The highest DR was recorded at the initial stage of drying due to a higher amount of moisture in the yam slice. Moisture diffusion was faster at the beginning stage of drying due to the available moisture in the surface of the slice, but the moisture diffusion reduced as drying progress. As the temperature was increased, the rate of drying increased while as slice thickness was increased the drying rate was reduced. In the initial drying stage falling rate was dominant indication moisture loss is controlled by diffusion, but at the middle to the end of the drying process, a constant rate was experienced [53]. This was in agreement with the findings reported by Harish et al. [54] for elephant foot yam, Ojediran et al., [8] for *Dioscorea rotundata* and Ononogbo et al., [32] for yam slices.

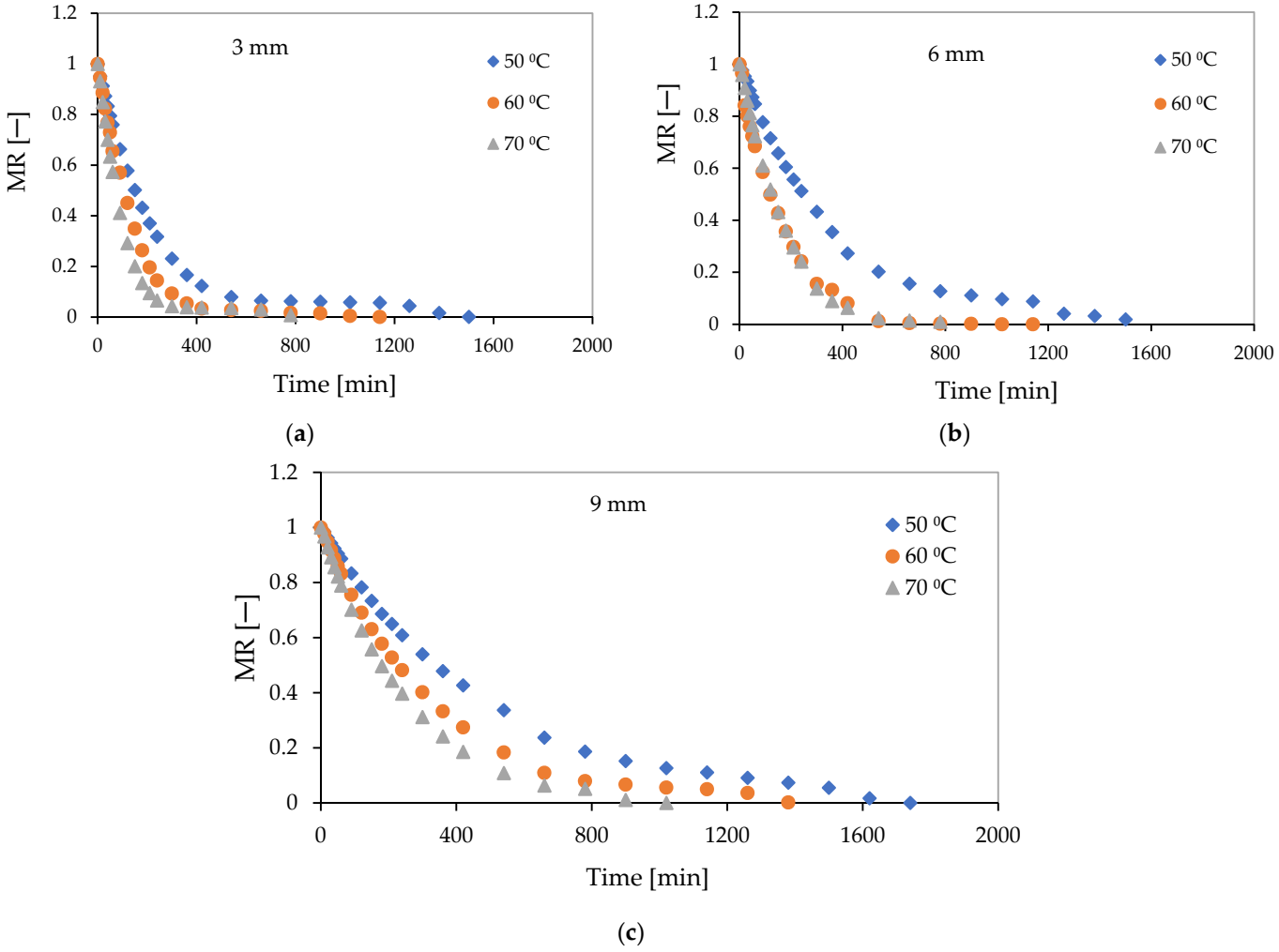

Figure 2. Drying curves of yam chips at different temperatures and slice thickness; (**a**) 3 mm, (**b**) 6 mm, and (**c**) 9 mm.

3.3. Moisture Diffusivity

The results of the moisture diffusivity (D_{eff}) are reported in Figure 4. The D_{eff} increased as drying temperature and slice thickness increased. The highest moisture diffusivity value was 4.2×10^{-8} m^2/s at the air temperature of 70 °C and the slices thickness of 9 mm while the lowest value was 2.7×10^{-9} m^2/s at the air temperature of 50 °C and the slice thickness of 3 mm. The increase in D_{eff} at higher temperature could be a result of destruction of the cell wall and a reduction in the moisture resistance ability of the yam slice. At the lower slice thickness, moisture diffusion is easier but augments with increase in thickness of the slices [8]. The D_{eff} range of most food products was between 10^{-12} and 10^{-8} m^2/s [55]. Similar D_{eff} range has been reported by many researchers such as in the researches of Harish et al., [54] for elephant foot yam (10^{-9} to 10^{-8} m^2/s), Fang et al. [33] for Chinese yam (10^{-9} m^2/s)and Geng et al., [56] for carrot(10^{-10} to 10^{-9} m^2/s).

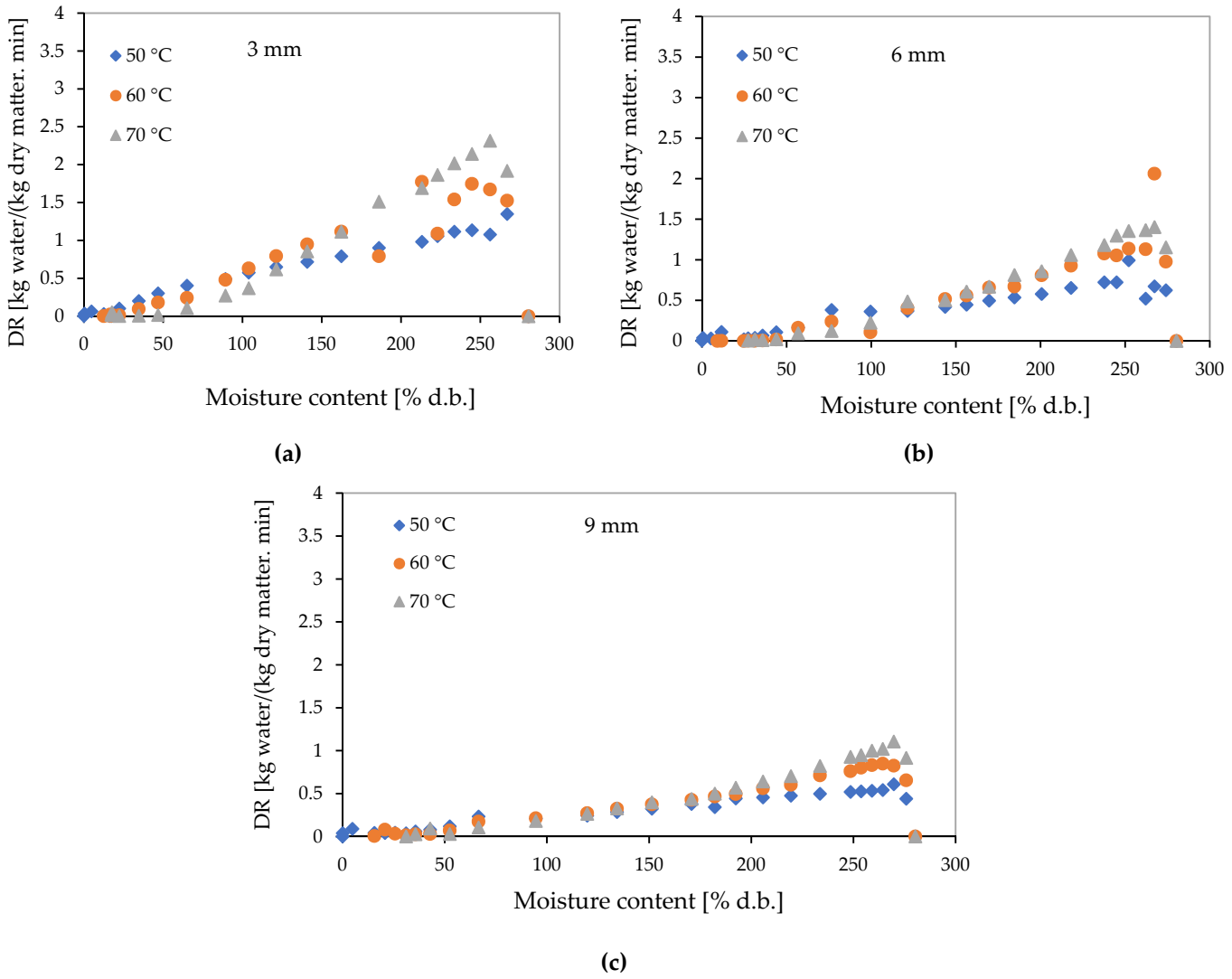

Figure 3. Drying rate curves of yam chips at different temperatures and slice thickness; (**a**) 3 mm, (**b**) 6 mm, and (**c**) 9 mm.

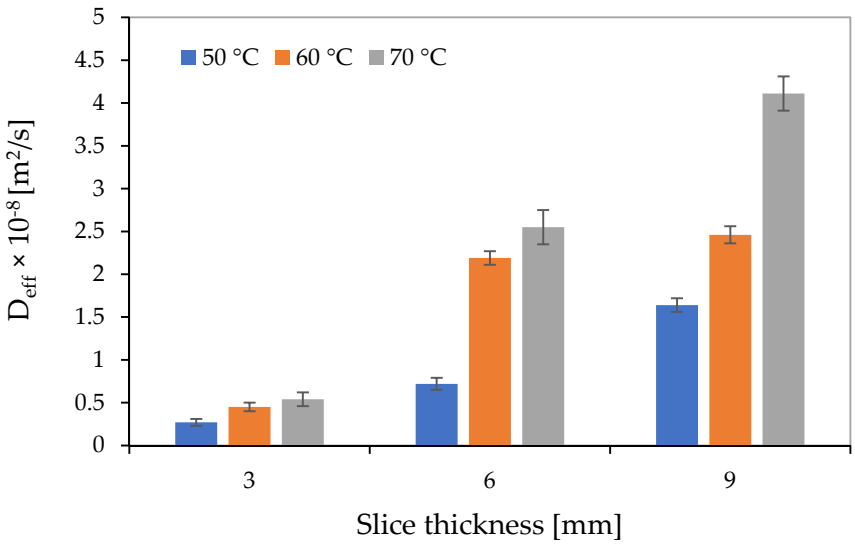

Figure 4. Moisture diffusivity as against slice thickness and temperature.

3.4. Activation Energy

Figure 5 shows the variation inactivation energy (E_a) with slice thickness. Activation energy ranged from 32 to 53 kJ/mol. The E_a increased with slice thickness. This signifies that more energy is required for moisture diffusion at higher slice thickness. A similar finding was reported by Ojediran et al., [8] for *Dioscorea rotundata* slices in a hot air dryer. Fang et al. [33] reported E_a for raw Chinese yam as 41.149 kJ/mol.

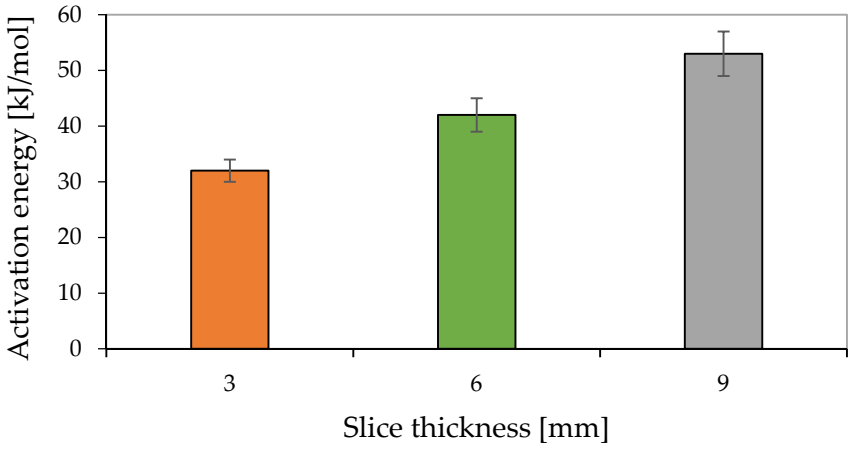

Figure 5. Activation energy as against slice thickness.

3.5. Mathematical Modelling of Drying Kinetic

The results of kinetic modelling using ten thin layer drying models are presented in Table 2 and Figure 6a–c. The most performed model was based on the R^2, RMSE, and SSE values. Several models, e.g., Midilli et al., logarithmic, approximation of diffusion, two-term, Page, Henderson and Pabis all performed well, but Midilli et al. was selected as the best model since it out-performed the other models used more frequently. The most correlation values were maximum coefficient of determination (R^2 = 0.9998), minimum root mean square error (RMSE = 0.0049), and minimum sum of square errors (SSE = 0.0023) for drying water yam slices in a convective hot air dryer. Moreover, Figure 5a–c further depicts the performance of Midilli et al. in predicting the drying behaviour of the yam slices in the hot air dryer. Midilli et al. has been selected by other authors for its high prediction ability; Chikpah et al., [57] for pumpkin drying in a convective dryer with different slice thicknesses, Hadjout-Krimat et al., [58] for pea pod drying in a microwave and convective dryer and Çetin [59] for orange slice drying in a convective dryer.

Table 2. Results of statistical analysis on the modelling of moisture ratio and drying time of water yam.

Drying Conditions	Model										
		1	**2**	**3**	**4**	**5**	**6**	**7**	**8**	**9**	**10**
50 °C + 3 mm	SSE	0.0122	0.0123	0.0123	0.0103	**0.0074**	0.0123	0.0122	0.7625	0.4036	0.0089
	R^2	0.9964	0.9964	0.9964	0.997	**0.9978**	0.9964	0.9964	0.7775	0.8822	0.9974
	RMSE	0.0217	0.0217	0.0213	0.0199	**0.0172**	0.0221	0.0226	0.1713	0.1271	0.0189
50 °C + 6 mm	SSE	0.0070	0.0073	0.0073	0.0059	0.0058	0.0056	**0.0051**	0.1945	0.1255	0.0064
	R^2	0.998	0.9979	0.9979	0.9983	0.9983	0.9984	**0.9985**	0.9436	0.9636	0.9981
	RMSE	0.0167	0.0171	0.0168	0.0153	0.0156	0.0153	**0.0150**	0.0882	0.0723	0.0163
50 °C + 9 mm	SSE	0.0032	0.0032	0.0032	0.0032	0.0030	**0.0021**	0.0032	0.0868	0.0561	0.0028
	R^2	0.9991	0.9991	0.9991	0.9991	0.9992	**0.9994**	0.9991	0.9757	0.9843	0.9992
	RMSE	0.0110	0.0110	0.0108	0.0110	0.0110	**0.0093**	0.0115	0.0578	0.0474	0.0107
60 °C + 3 mm	SSE	0.0038	0.0068	0.0084	0.0037	0.0068	0.0065	0.0068	0.6086	0.3402	**0.0035**

Table 2. *Cont.*

Drying Conditions	Model										
		1	**2**	**3**	**4**	**5**	**6**	**7**	**8**	**9**	**10**
60 °C + 6 mm	R^2	0.9987	0.9976	0.9971	0.9987	0.9976	0.9977	0.9976	0.7878	0.8814	**0.9988**
	RMSE	0.0135	0.0180	0.0196	0.0133	0.0184	0.018	0.0189	0.1702	0.1304	**0.0132**
	SSE	0.0063	0.0062	0.0076	0.0075	0.0059	**0.0050**	0.0062	0.516	0.2368	0.0060
60°C + 9 mm	R^2	0.9978	0.9979	0.9974	0.9974	0.998	**0.9983**	0.9979	0.8207	0.9177	0.9979
	RMSE	0.0170	0.0168	0.0181	0.0184	0.0168	**0.0155**	0.0176	0.1531	0.1062	0.0169
	SSE	**0.0018**	**0.0018**	0.0019	0.0019	0.0018	0.0019	0.0018	0.1275	0.0785	0.0018
70 °C + 3 mm	R^2	**0.9994**	**0.9994**	0.9994	0.9994	0.9994	0.9994	0.9994	0.9594	0.975	0.9994
	RMSE	**0.0090**	**0.0090**	0.0088	0.0090	0.0091	0.0092	0.0093	0.0745	0.0597	0.0091
	SSE	0.0041	0.0071	0.0099	0.0059	0.0066	0.0088	0.0037	0.5434	0.3082	**0.0023**
70 °C + 6 mm	R^2	0.9983	0.997	0.9958	0.9975	0.9972	0.9963	0.9984	0.7717	0.8706	**0.999**
	RMSE	0.0150	0.0198	0.0228	0.0181	0.0197	0.0227	0.0153	0.1738	0.1346	**0.0115**
	SSE	0.0013	0.0043	0.0064	**0.0008**	0.0034	0.0009	0.0010	0.1725	0.1108	0.0013
70 °C + 9 mm	R^2	0.9995	0.9984	0.9976	**0.9997**	0.9987	0.9996	0.9996	0.9355	0.9586	0.9995
	RMSE	0.0082	0.0150	0.0179	**0.0066**	0.0137	0.0072	0.0075	0.0953	0.0785	0.0084
	SSE	0.0010	0.0012	0.0012	0.0007	**0.0005**	0.0012	0.0012	0.0898	0.0533	**0.0005**
	R^2	0.9996	0.9996	0.9995	0.9997	**0.9998**	0.9995	0.9996	0.9662	0.98	**0.9998**
	RMSE	0.0070	0.0077	0.0076	0.0059	**0.0049**	0.0080	0.0080	0.067	0.0529	**0.0049**

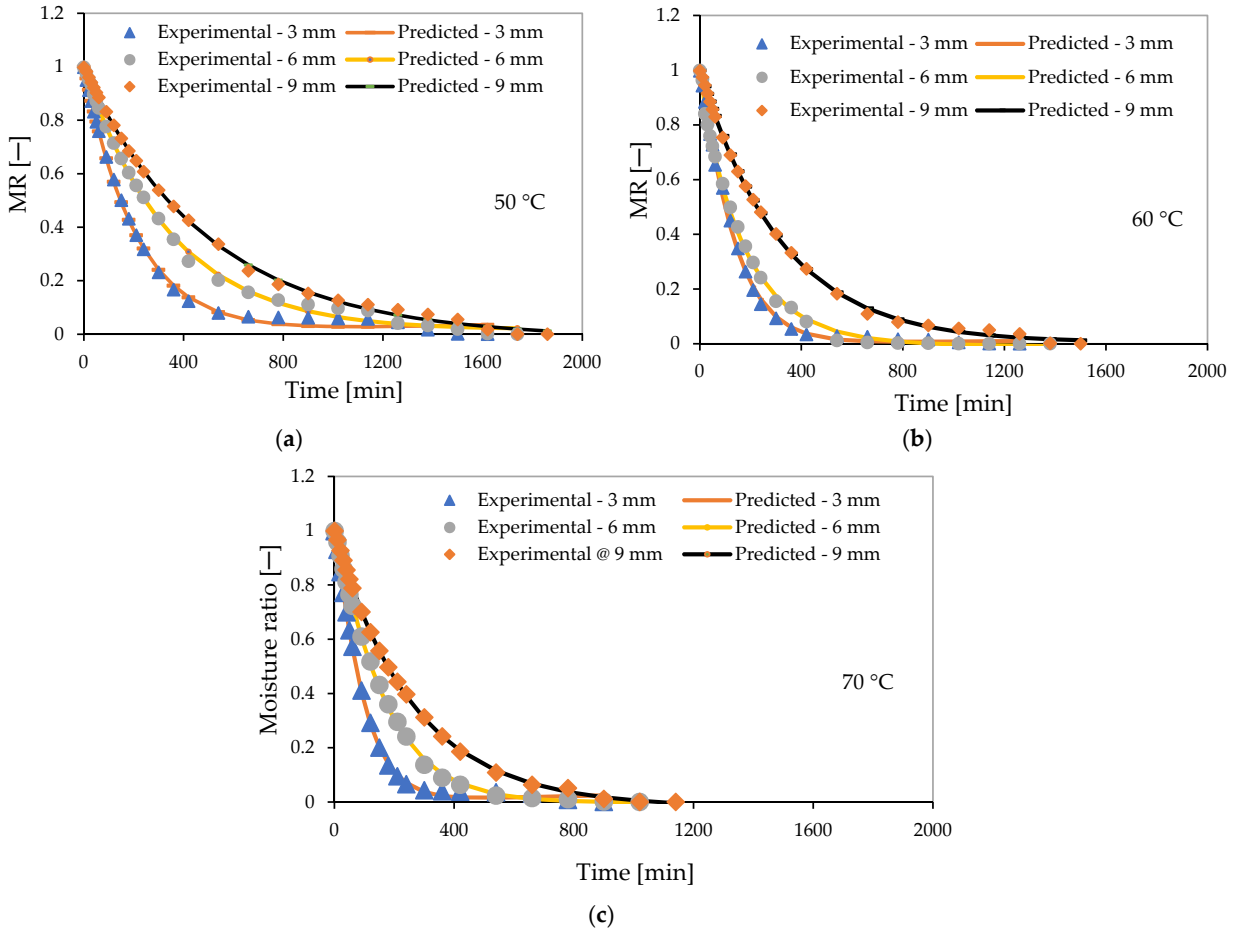

Figure 6. Validation in moisture ratios of the Midilli et al. model with drying time for yam slices at varying temperatures; (**a**) 50 °C, (**b**) 60 °C, and (**c**) 70 °C.

3.6. Uncertainty Analyses

The results of the uncertainties are as shown in Table 3. It was observed that the uncertainty percentage for both the experiment measurements and the calculated or predicted values were all lower than 5%, which was within the acceptable range. These results agree with the findings observed by other researchers such as Akpinar et al. [16], Beigi et al. [17], Liu et al. [22] and Zohrabi et al. [51].

Table 3. Uncertainties of the experimental measurements and overall uncertainties for predicted energetic and exergetic responses.

Parameters	Unit	Uncertainty (%)
Experimental measurements		
Drying air temperature	°C	±0.5
Drying air relative humidity	%	±1.0
Product weight loss	g	±0.0001
Process time	s	±3.0
Drying air velocity	m/s	±0.52
Predicted drying kinetic responses		
Moisture ratio	Dimensionless	±1.46
Effective diffusivity	m^2/s	±2.66
Activation energy	kJ/mol	±2.89
Predicted energetic responses		
Mass flow rate	kg/s	±0.63
Energy utilization	J/s	±1.43
Energy utilization ratio	Dimensionless	±3.84
Energy efficiency	%	±2.21
Predicted exergetic responses		
Exergy inflow	J/s	±1.35
Exergy outflow	J/s	±1.68
Exergy loss	J/s	±2.65
Exergy efficiency	%	±2.33
Improvement potential	J/s	±2.77
Exergetic sustainability index	Dimensionless	±2.98

3.7. Energy Evaluation

3.7.1. Energy Utilization

The result of the energy utilization (EU) as a function of air temperature and slice thickness of the water yam is represented in Figure 7. EU varied from 10 to 150 J/s for all parameters considered. EU increased during the drying process by an increase in temperature (50 to 70 °C). This was due to high input enthalpy and fast heat and mass transfer rate [60]. This result is compatible with the results observed by Aviara et al., [15] for hot air drying of cassava starch, Beigi et al. [17] for deep bed convective drying of rough rice, Okunola et al. [61] for forced convection cabinet drying of okra, and Liu et al. [22] for hot air impingement drying of mushroom slice. Additionally, EU increased by an increase in the slice thickness (3 to 9 mm) (Figure 7). This is due to the increase in volume of the slice requiring more energy consumption for moisture transport through pores of the product [62]. A similar result was reported by Liu et al. [22] for hot air impingement drying of mushroom slices.

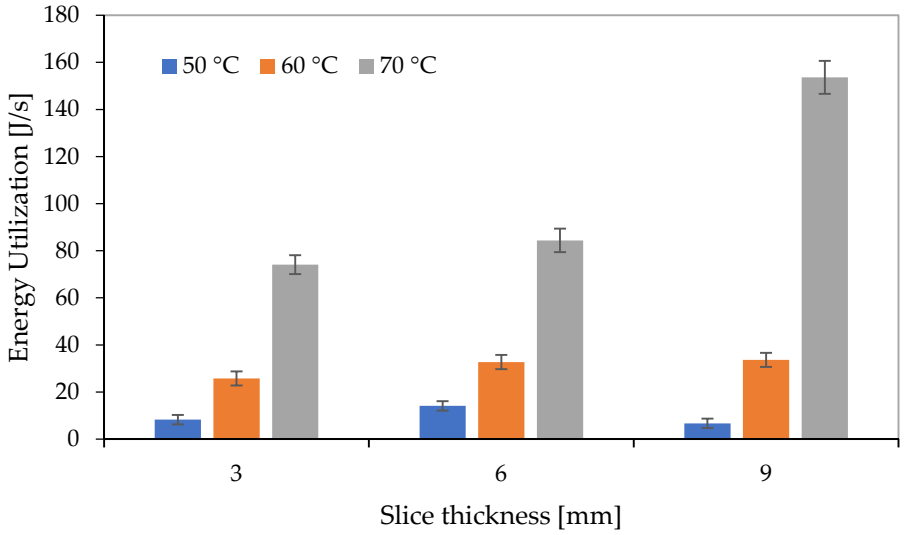

Figure 7. Energy utilization analysis of water yam in a hot air dryer as affected by temperature and slice thickness.

3.7.2. Energy Utilization Ratio

The relationships between energy utilization ratio (EUR), air temperature, and slice thickness are shown in Figure 8. EUR varied from 0.39 to 0.79 for all the temperature and slice thickness levels considered. In addition, EUR increased by an increase in the temperature levels (50 to 70 °C). This is because at high temperatures there is more transfer of heat between the walls of the dryer, thereby increasing moisture evaporation rate from the product [22]. This observation was in agreement with previous work by Aghbashlo et al. [19] for thin layer drying of potato in a continuous band dryer and Liu et al. [22] for hot air impingement drying of mushroom slice. Moreover, EUR increased by an increase in slice thickness (3 to 6 mm), but from slice thickness of 6 to 9 mm EUR decreased at 50 and 60 °C and a slightly increased at 70 °C (Figure 8). This observation was similar with the findings in the study of Liu et al. [22] for hot air impingement for drying of mushroom slices.

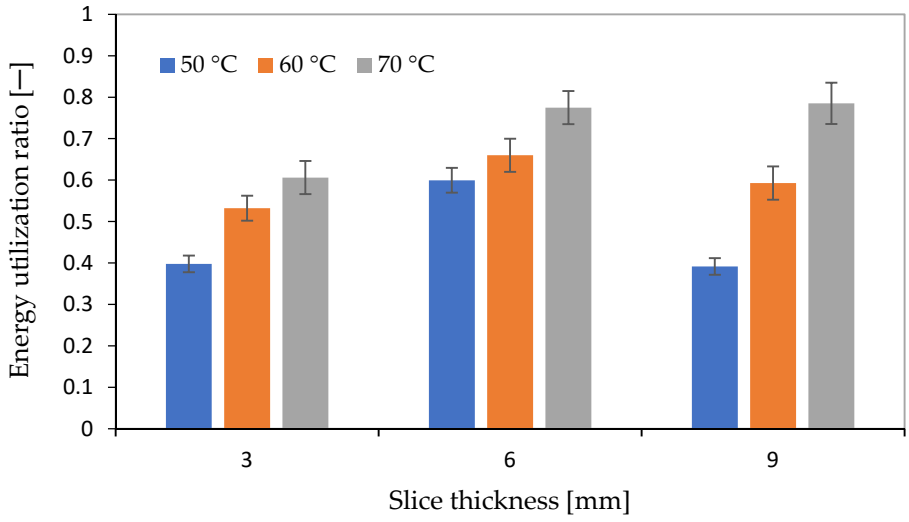

Figure 8. Energy utilization ratio analysis of water yam in a hot air dryer as affected by temperature and slice thickness.

3.8. Energy Evaluation

3.8.1. Exergy Inflow, Exergy Outflow and Exergy Loss

The variations in exergy inflow (EX_1), exergy outflow (EX_2), and exergy loss (EX_L) with temperature and slice thickness levels of the yam slices in a convective hot air dryer are presented in Figure 9. The highest EX_1, EX_2, and EX_L were 30, 17.5, and 12.5 J/s, respectively which were recorded at 70 °C and slice thickness of 9 mm, and the lowest values were 8, 6 and 2 J/s, respectively which were achieved at 50 °C and slice thickness of 9 mm. The findings showed that EX_1, EX_2, and EX_L increased by an increase in temperature from 50 to 70 °C. This signifies that the more energy supplied by the dryer at high temperature is not fully utilized by the product during drying experiment [22]. This finding was consistent with several studies, such as the results of Akpinar et al. [16] for convective hot air drying of red pepper, Corzo et al. [23] for thin layer drying of coroba slice, Beigi et al. [17] for deep bed convective drying of rough rice, Castro et al. [28] for convective drying of onion slice, and Liu et al. [22] for hot air impingement drying of mushroom slice. In addition, EX_1, EX_2, and EX_L slightly increased for bigger slice thickness, although at 50 °C, EX_1, EX_2, and EX_L decreased slightly with sample thickness. The increase in EX_L was due to more moisture evaporation, which caused a reduction in exergy at the outlet airflow. A similar finding was reported by Liu et al. [22] for hot air impingement drying of mushroom slice.

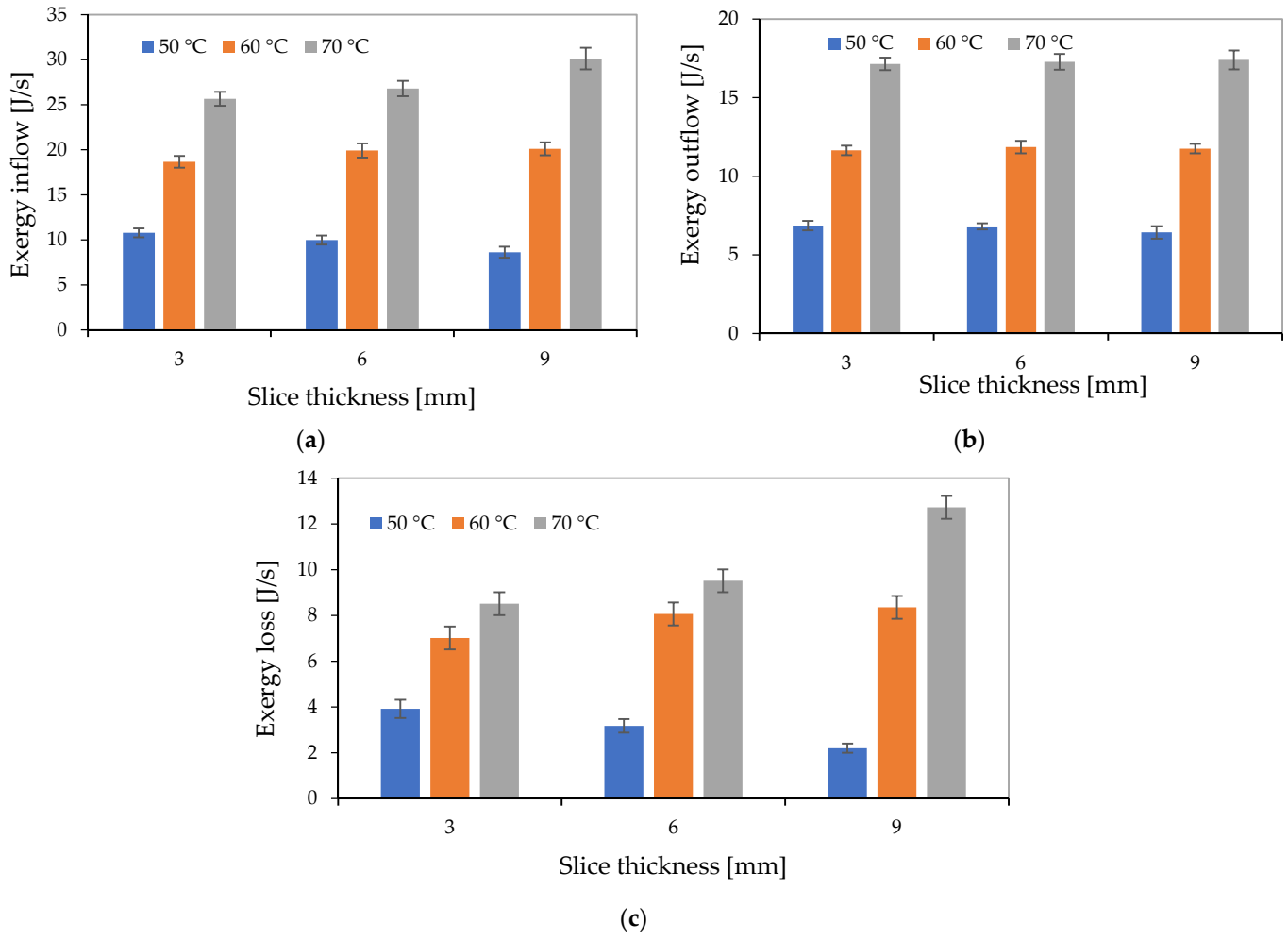

Figure 9. Exergy analyses of water yam in a hot air dryer as affected by temperature and slice thickness; (**a**) exergy inflow, (**b**) exergy outflow, (**c**) exergy loss.

3.8.2. Exergy Efficiency

The result of the exergy efficiency (EX_{eff}) is shown in Figure 10. EX_{eff} ranged between 58 and 75% for all drying parameters. The highest EX_{eff} was at 70 °C and slice thickness of 9 mm, while the lowest EX_{eff} was at 50 °C and same thickness. The EX_{eff} of the sample increased by an increase in temperature (50 to 70 °C). EX_{eff} in a thermodynamic system is evaluated by the exergy of the air at the outlet of the drying system. The outlet exergy either increases or reduces the EX_{eff}. An increase in exergy efficiency was expected due to the fact of higher exergy loss at higher temperature [23]. This finding was in agreement with ones Colak and Hepbasli [63] reported for tray drying of green olive, Aviara et al. [15] for tray drying of cassava starch, and Okunola et al. [61] for forced convection cabinet drying of okra. Additionally, EX_{eff} was slightly decreased by an increase in slice thickness for 50 and 60 °C temperature, whereas for 70 °C, EX_{eff} increased with sample thickness. The decrease in EX_{eff} is as a result of higher exergy loss experienced on larger sample thickness. Similar decrease in EX_{eff} as a function of sample thickness was reported by Liu et al. [22] for hot air impingement drying of mushroom slice at a constant temperature of 65 °C and also the study conducted by Darvishi et al. [26] for microwave drying of kiwi slice.

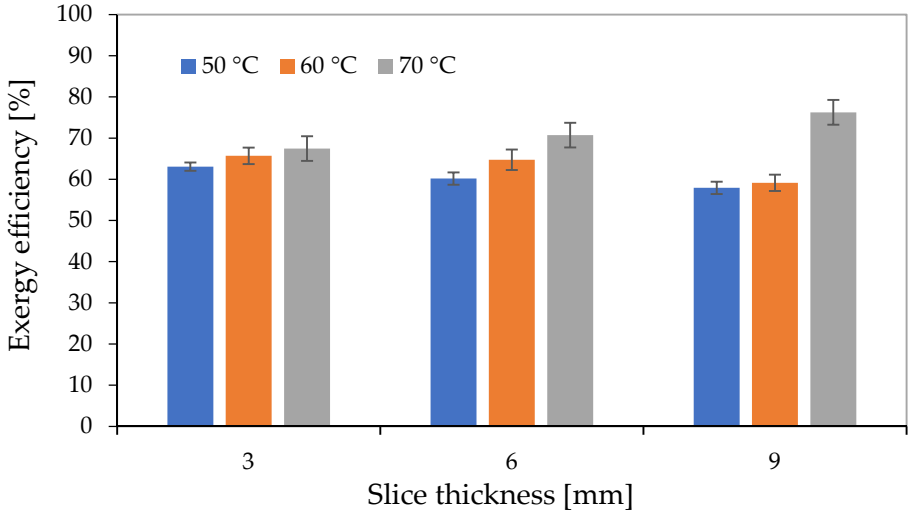

Figure 10. Exergy efficiency of water yam in a hot air dryer as affected by temperature and slice thickness.

3.8.3. Improvement Potential

Figure 11 shows the variation in improvement potential (IP) with drying air temperature and sample slice thickness. The IP ranged from 0.7 to 5.5 J/s. The highest IP was observed at slice thickness of 9 mm and air temperature of 70 °C, while the lowest IP was at slice thickness of 9 mm and air temperature of 50 °C. IP of the hot air dryer increased by an increase in drying air temperature (50 to 70 °C). A similar trend was reported by Icier et al. [24] for tray drying of broccoli florets, Aghbashlo et al. [20] for spray drying of fish oil microencapsulation, Aviara et al. [15] for tray drying of cassava starch, and Beigi et al. [17] for deep bed convective drying of rough rice. The IP of the dryer increased by an increase in sample thickness for temperature of 60 and 70 °C, but for 50 °C, IP decreased by an increase in sample thickness.

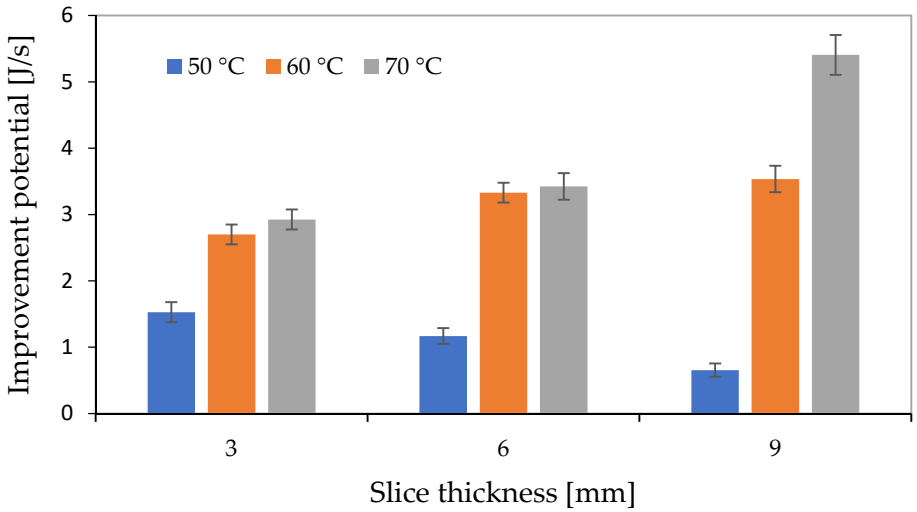

Figure 11. Improvement potential of water yam in a hot air dryer as affected by temperature and slice thickness.

3.8.4. Exergetic Sustainability Index

The relationship between exergetic sustainability index (ESI), drying air temperature and slice thickness are presented in Figure 12. As shown, the highest ESI was found 5.3 at 70 °C and slice thickness of 9 mm, while the lowest ESI was 2.5 at 50 °C and slice thickness of 9 mm. An increase in drying air temperature increased the ESI. Therefore, it is advised to enhance the exergy efficiency of energy intensive process so as to reduce the environmental impact. Beigi et al. [17] reported that higher temperature increases the ESI of deep bed drying of rough rice in a convective dryer. ESI decreased by an increase in slice thickness for 50 and 60 °C, but for 70 °C ESI increased with slice thickness.

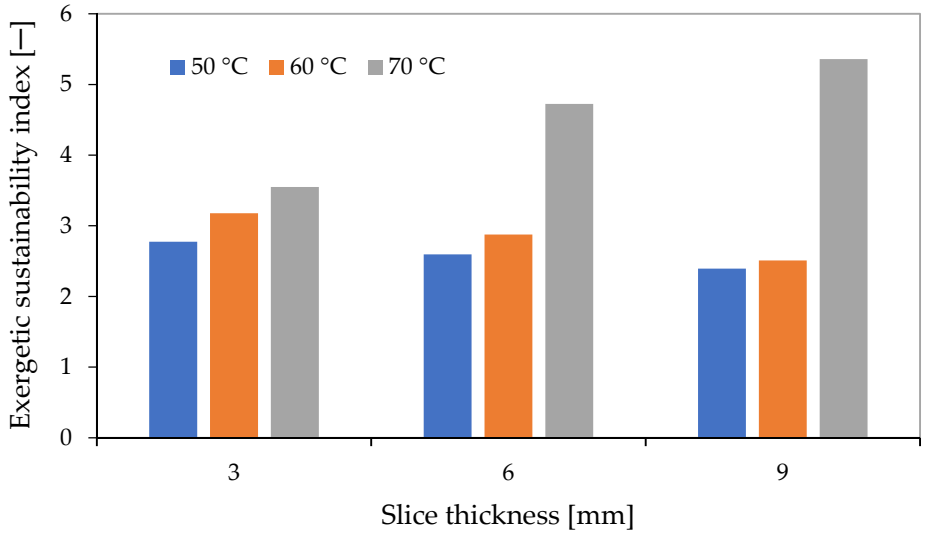

Figure 12. Exergetic sustainability index of water yam in a hot air dryer as affected by temperature and slice thickness.

4. Conclusions

In this study, the effect of air temperature and slice thickness on drying characteristics, energy, and exergy parameters using a hot air dryer was investigated for water yam. The results revealed that Midilli amongst the several mathematical models used had the best prediction of the thin layer drying kinetics for water yam with R^2, RMSE, and SSE values of 0.9998, 0.0049, and 0.0023, respectively. D_{eff} increased with drying air temperature and

slice thickness, while E_a increased with slice thickness. Increasing the air temperature and decreasing the slice thickness levels increased the drying rate and reduced the drying time. Increasing the temperature increased the EU, EUR, EX_1, EX_2, EX_L, EX_{eff}, IP, and ESI, while increasing the slice thickness showed a fluctuating effect on the energy and exergy parameters. EU, EUR, EX_L and EX_{eff} varied from 10 to 150 J/s, 0.39 to 0.79, 2 to 12.5 J/s and 58 to 75%, respectively. In addition, IP and ESI were in the range of 0.7 to 5.5 J/s and 2.5 to 5.3. Energy and exergy analyses is important for eliminating system losses during drying and in optimization of the performance regarding the drying process of water yam in a convective hot air dryer. Finally, to improve the thermodynamic performance and reduce the harmful environmental effects of the process, higher hot air temperatures and thinner samples should be used.

Author Contributions: Conceptualization, C.E.O. and M.S.; methodology, A.A.O. and M.K.; software, T.A.A., M.K. and C.E.O.; validation, E.O.I., A.T.O. and C.E.O.; formal analysis, M.K. and C.E.O.; investigation, E.O.I., C.E.O. and A.T.O.; resources, A.T.O., M.K. and M.S.; data curation, C.E.O. and A.T.O.; writing—original draft preparation, C.E.O., A.A.O. and T.A.A.; writing—review and editing, M.K., M.S., E.O.I. and K.W. visualization, A.T.O.; supervision, C.E.O. and A.A.O. All authors have read and agreed to the published version of the manuscript.

Funding: This research received no external funding.

Data Availability Statement: The datasets generated during and/or analysed during the current study are available from the corresponding author on reasonable request.

Conflicts of Interest: The authors declare that they have no known competing financial interests or personal relationships that could have appeared to influence the work reported in this paper.

Nomenclature

C_{pA2}	Specific heat of the outlet air [J/kg]
E_1	Energy input (J/s)
E_2	Energy output (J/s)
C_{pA1}	Specific heat of the inlet air [J/kg]
C_{pA}	Specific heat [J/kg]
DR	Drying rate [kg water/(kg dry matter*min]
D_{eff}	Moisture diffusivity [m^2/s]
D_o	Arrhenius equation pre-exponential factor, [m^2/s],
E_a	Activation energy [kJ/mol]
EU	Energy utilization [J/s]
EX	Exergy [J/s]
EX_1	Exergy inflow [J/s]
EX_L	Exergy loss [J/s]
EX_{eff}	Exergy efficiency [%]
EX_2	Exergy outflow [J/s]
g	Gravity [J/kg]
h	Enthalpy [J/kg]
H	Humidity ratio
h_{sat}	Saturated vapor enthalpy [J/kg]
h_1 and h_2	Enthalpy of the air at dryer inlet temperature and outlet dryer temperature [J/kg], respectively.
h_∞	Ambient air enthalpy [J/kg]
I_p	Improvement potential [J/s]
k, k_1, k_2, g, h, a, b, c,	Drying rate constant
L	Half slab thickness [m]
M_t	Moisture content dry basis at any time t [%]
M_o	Initial moisture content [% dry basis]
MR	Moisture ratio [-]
$M_{t+\Delta t}$	Moisture content at t+Δt
MR_{pre}	Predicted moisture ratio

MR_{exp}	Experimental moisture ratio
MR_{AVper}	Average predicted moisture ratio
$\dot{M}_{A1}$, and $\dot{M}_{A2}$	Mass flow rate of air at inlet and outlet points [kg/s], respectively
$\dot{M}_A$	Mass flow rate [kg/s]
N	Number of data points
$P_\infty[V - V_\infty]$	Work [J/kg]
Q	Heat energy gained by the system [J/s]
R	Universal gas constant, [8.3143 kJ/mol K]
RMSE	Root mean square error
R^2	Coefficient of determination
$S - S_\infty$	Entropy [J/kg]
SSE	Sum of squared errors
T_{dA}	Temperature (°C)
T_{dA2}	Temperature of drying air at the outlet [°C]
T_{dA1}	Temperature of drying air at inlet [°C]
T_o	Ambient temperature (°C)
t	Time [min]
$U - U_\infty$	Internal energy [J/kg]
U	Stands for uncertainty level of the result.
$u_1, u_2, u_3, \ldots \ldots u_n$	Uncertainties in the independent variables
$\frac{v^2}{2}$	Momentum
v_1 and v_2	Velocities of the air at inlet and outlet [m/s], respectively.
$\dot{V}_A$	Volumetric flow rate [m^3/s]
W	Mechanical work done per time [J/s]
W_t	Weight of sample at time, t [g]
W_d	Weight of sample at dynamic equilibrium [g]
$x_1, x_2, x_3, \ldots \ldots x_n$	Independent variables
y	function of independent variables
ΔU	Internal energy [J/s]
Δt	Change in time [min]
ρ_A	density [kg/m^3]

References

1. Otegbayo, B.O.; Oguniyan, D.J.; Olunlade, B.A.; Oroniran, O.O.; Atobatele, O.E. Characterizing genotypic variation in biochemical composition, anti-nutritional and mineral bioavailability of some Nigerian yam (*Dioscorea* spp.) land races. *J. Food Sci. Technol.* **2017**, *55*, 205–216. [CrossRef] [PubMed]
2. Srikanth, K.S.; Sharanagat, V.S.; Kumar, Y.; Bhadra, R.; Singh, L.; Nema, P.K.; Kumar, V. Convective drying and quality attributes of elephant foot yam (*Amorphophallus paeoniifolius*). *LWT* **2019**, *99*, 8–16. [CrossRef]
3. Nwafor, J.O.; Kanu, A.N.; Kelechukwu, E.C.; Nwohu, N.O.; Ezebuiro, V.N. Physico-chemical properties of water yam and cowpea flour blends for production of snacks. *South Asian J. Res. Microbiol.* **2020**, 1–8. [CrossRef]
4. Otunola, G.A.; Afolayan, A.J. Evaluation of the physicochemical, proximate, and sensory properties of moinmoin from blends of cowpea and water yam flour. *Food Sci. Nut.* **2018**, *6*, 991–997. [CrossRef] [PubMed]
5. Chen, X.; Lu, J.; Li, X.; Wang, Y.; Miao, J.; Mao, X.; Zhao, C.; Gao, W. Effect of blanching and drying temperatures on starch-related physicochemical properties, bioactive components and antioxidant activities of yam flours. *LWT* **2017**, *82*, 303–310. [CrossRef]
6. Huang, Y.; Min, Z.; Mujumdar, A.S.; Luo, Z.; Fang, Z. Dehydrated fruits and vegetables using low temperature drying technologies and their application in functional beverages: A review. *Drying Technol.* **2022**. [CrossRef]
7. Wang, D.; Zhang, M.; Ju, R.; Mujumdar, A.S.; Yu, D. Novel drying techniques for controlling microbial contamination in fresh food: A review. *Drying Technol.* **2022**. [CrossRef]
8. Ojediran, J.O.; Okonkwo, C.E.; Adeyi, A.J.; Adeyi, O.; Olaniran, A.F.; George, N.E.; Olayanju, A.T. Drying characteristics of yam slices (Dioscorearotundata) in a convective hot air dryer: Application of ANFIS in the prediction of drying kinetics. *Heliyon* **2020**, *6*, e03555. [CrossRef] [PubMed]
9. Çetin, N.; Ciftci, B.; Kara, K.; Kaplan, M. Effects of gradually increasing drying temperatures on energy aspects, fatty acids, chemical composition, and in vitro ruminal fermentation of acorn. *Environ. Sci. Pollution. Res.* **2022**, 1–17. [CrossRef] [PubMed]
10. Golpour, I.; Kaveh, M. Blanco-Marigorta, A.M.; Marcos, J.D.; Guiné, R.P.F.; Chayjan, R.A.; Khalife, E.; Karami, H. Multi-response design optimisation of a combined fluidized bed-infrared dryer for terebinth (*Pistacia atlantica* L.) fruit drying process based on energy and exergy assessments by applying RSM-CCD modelling. *Sustainability* **2022**, *14*, 15220.
11. Kamal, M.M.; Ali, M.R.; Shishir, M.R.; Mondal, S.C. Thin-layer drying kinetics of yam slices, physicochemical, and functional attributes of yam flour. *J. Food Process. Eng.* **2020**, *43*, e13448. [CrossRef]

12. Kumar, A.; Ramakumar, P.; Patel, A.A.; Gupta, V.K.; Singh, A.K. Influence of drying temperature on physico-chemical and techno-functional attributes of elephant foot yam (*Amorphophallus paeoniifolius*) var. Gajendra. *Food Biosci.* **2016**, *16*, 11–16. [CrossRef]
13. Ren, F.; Perussello, C.A.; Zhang, Z.; Gaffney, M.T.; Kerry, J.P.; Tiwari, B.K. Enhancement of phytochemical content and drying efficiency of onions (*Allium cepa* L.) through blanching. *J. Sci. Food Agri.* **2017**, *98*, 1300–1309. [CrossRef]
14. Ju, H.Y.; Zhang, Q.; Mujumdar, A.S.; Fang, X.M.; Xiao, H.W.; Gao, Z.J. Hot-air drying kinetics of yam slices under step change in relative humidity. *Int. J. Food Eng.* **2016**, *12*, 783–792. [CrossRef]
15. Aviara, N.A.; Onuoha, L.N.; Falola, O.E.; Igbeka, J.C. Energy and exergy analyses of native cassava starch drying in a tray dryer. *Energy* **2014**, *73*, 809–817. [CrossRef]
16. Akpinar, E.K. Energy and exergy analyses of drying of red pepper slices in a convective type dryer. *Int. Commun. Heat Mass Transfer.* **2004**, *31*, 1165–1176. [CrossRef]
17. Beigi, M.; Tohidi, M.; Torki-Harchegani, M. Exergetic analysis of deep-bed drying of rough rice in a convective dryer. *Energy* **2017**, *140*, 374–382. [CrossRef]
18. Chowdhury, M.M.I.; Bala, B.K.; Haque, M.A. Energy and exergy analysis of the solar drying of jackfruit leather. *Biosys. Eng.* **2011**, *110*, 222–229. [CrossRef]
19. Aghbashlo, M.; Kianmehr, M.H.; Arabhosseini, A. Energy and Exergy Analyses of Thin-Layer Drying of Potato Slices in a Semi-Industrial Continuous Band Dryer. *Drying Technol.* **2008**, *26*, 1501–1508. [CrossRef]
20. Aghbashlo, M.; Mobli, H.; Rafiee, S.; Madadlou, A. Energy and exergy analyses of the spray drying process of fish oil microencapsulation. *Biosys. Eng.* **2012**, *111*, 229–241. [CrossRef]
21. Sami, S.; Etesami, N.; Rahimi, A. Energy and exergy analysis of an indirect solar cabinet dryer based on mathematical modeling results. *Energy* **2011**, *36*, 2847–2855. [CrossRef]
22. Liu, Z.-L.; Bai, J.-W.; Wang, S.-X.; Meng, J.S.; Wang, H.; Yu, X.L.; Gao, Z.J.; Xiao, H.W. Prediction of energy and exergy of mushroom slices drying in hot air impingement dryer by artificial neural network. *Drying Technol.* **2019**, 1–12. [CrossRef]
23. Corzo, O.; Bracho, N.; Vásquez, A.; Pereira, A. Energy and exergy analyses of thin layer drying of coroba slices. *J. Food Eng.* **2008**, *86*, 151–161. [CrossRef]
24. Icier, F.; Colak, N.; Erbay, Z.; Kuzgunkaya, E.H.; Hepbasli, A. A comparative study on exergetic performance assessment for drying of broccoli florets in three different drying systems. *Drying Technol.* **2010**, *28*, 193–204. [CrossRef]
25. Akbulut, A.; Durmuş, A. Energy and exergy analyses of thin layer drying of mulberry in a forced solar dryer. *Energy* **2010**, *35*, 1754–1763. [CrossRef]
26. Darvishi, H.; Zarein, M.; Farhudi, Z. Energetic and exergetic performance analysis and modeling of drying kinetics of kiwi slices. *J. Food Sci. Technol.* **2016**, *53*, 2317–2333. [CrossRef] [PubMed]
27. Surendhar, A.; Sivasubramanian, V.; Vidhyeswari, D.; Deepanraj, B. Energy and exergy analysis, drying kinetics, modeling and quality parameters of microwave-dried turmeric slices. *J. Therm. Analysis Calorim.* **2018**, *136*, 185–197. [CrossRef]
28. Castro, M.; Román, C.; Echegaray, M.; Mazza, G.; Rodriguez, R. Exergy Analyses of Onion Drying by Convection: Influence of Dryer Parameters on Performance. *Entropy* **2018**, *20*, 310. [CrossRef] [PubMed]
29. Argo, B.D.; Ubaidillah, U. Thin-layer drying of cassava chips in multipurpose convective tray dryer: Energy and exergy analyses. *J. Mechanical. Sci. Technol.* **2020**, *34*, 435–442. [CrossRef]
30. Parhizi, Z.; Karami, H.; Golpour, I.; Kaveh, M.; Szymanek, M.; Blanco-Marigorta, A.M.; Marcos, J.D.; Khalife, E.; Skowron, S.; Othman, N.A.; et al. Modeling and Optimization of Energy and Exergy Parameters of a Hybrid-Solar Dryer for Basil Leaf Drying Using RSM. *Sustainability* **2022**, *14*, 8839. [CrossRef]
31. Horwitz, W. *Official Methods of Analysis*; Association of Official Analytical Chemist: Washington, DC, USA, 1990; Volume 222, pp. 30–40.
32. Ononogbo, C.; Nwakuba, N.R.; Nwaji, G.N.; Nwufo, O.C.; Nwosu, E.C.; Okoronkwo, C.A.; Igbokwe, J.O.; Anyanwu, E.E. Thermal efficiency and drying behaviour of yam slices in a dryer driven by the waste heat of exhaust gases. *Sci. Afr.* **2020**, *17*, e01310. [CrossRef]
33. Fang, S.; Wang, L.-P.; Wu, T. Mathematical modeling and effect of blanching pretreatment on the drying kinetics of Chinese yam (Dioscoreaopposita). *Chem. Ind. Chem. Eng. Q.* **2015**, *21*, 511–518. [CrossRef]
34. Omari, A.; Behroozi-Khazaei, N.; Sharifian, F. Drying kinetic and artificial neural network modeling of mushroom drying process in microwave-hot air dryer. *J. Food Process. Eng.* **2018**, *41*, e12849. [CrossRef]
35. Zadhossein, S.; Abbaspour-Gilandeh, Y.; Kaveh, M.; Kalantari, D.; Khalife, E. Comparison of two artificial intelligence methods (ANNs and ANFIS) for estimating the energy and exergy of drying cantaloupe in a hybrid infrared-convective dryer. *J. Food Process. Preserv.* **2022**, *46*, e16836. [CrossRef]
36. Sharifian, F.; Nikbakht, A.M.; Arefi, A.; Modarres Motlagh, A. Experimental assessment of energy and mass transfer in microwave drying of fig fruit. *J. Agr. Sci. Tech.* **2015**, *17*, 1695–1705.
37. Sridhar, K.; Charles, A.L. Mathematical modeling and effect of drying temperature on physicochemical properties of new commercial grape "Kyoho" seeds. *J. Food Process. Eng.* **2019**, *43*, e13203. [CrossRef]
38. Pandiselvam, R.; Aydar, A.Y.; Kutlu, N.; Aslam, R.; Sahni, P.; Mitharwal, S.; Gavahian, M.; Kumar, M.; Raposo, A.; Yoo, S.; et al. Individual and interactive effect of ultrasound pre-treatment on dryingkinetics and biochemical qualities of food: A critical review. *Ultrason. Sonochem.* **2023**, *92*, 106261. [CrossRef] [PubMed]

39. Meng, Z.; Cui, X.; Zhang, H.; Liu, Y.; Wang, Z.; Zhang, F. Study on drying characteristics of yam slices under heat pump-electrohydrodynamics combined drying. *Case Stud. Therm. Eng.* **2023**, *41*, 102601. [CrossRef]
40. Çetin, N. Comparative assessment of energy analysis, drying kinetics, and biochemical composition of tomato waste under different drying conditions. *Sci. Hortic.* **2022**, *305*, 111405. [CrossRef]
41. Doymaz, I. Influence of infrared drying on some quality properties of nashi pear (Pyruspyrifolia) slices. *Erwerbs-Obstbau* **2022**, *65*, 47–54. [CrossRef]
42. Pradechboon, T.; Dussadee, N.; Unpaprom, Y.; Chindaraksa, Y. Effect of rotary microwave drying on quality characteristics and physical properties of Kaffir lime leaf (Citrus hystrix D.C.). *Biomass. Convers. Biorefin.* **2022**. [CrossRef]
43. Kumar, A.; Kandasamy, P.; Chakraborty, I.; Hangshing, L. Analysis of energy consumption, heat and mass transfer, drying kinetics and effective moisturediffusivity during foam-mat drying of mango in aconvective hot-air dryer. *Biosys. Eng.* **2022**, *219*, 85–102. [CrossRef]
44. EL-Mesery, H.S.; Tolba, N.M.; Kamel, R.M. Mathematical modelling and performance analysis of airflow distribution systems inside convection hot-air dryers. *Alex. Eng. J.* **2023**, *62*, 237–256. [CrossRef]
45. Doymaz, İ. Infrared drying of sweet potato (*Ipomoea batatas* L.) slices. *J. Food Sci. Technol.* **2011**, *49*, 760–766. [CrossRef] [PubMed]
46. Doymaz, İ. Infrared drying of kiwifruit slices. *Int. J. Green Energy.* **2018**, *15*, 622–628. [CrossRef]
47. Zia, S.; Khan, M.R.; Aadil, R.M. Kinetic modeling of different drying techniques and their influence on color, bioactive compounds, antioxidant indices and phenolicprofile of watermelon rind. *J. Food Meas Charact.* **2023**, *17*, 1068–1081. [CrossRef]
48. Hazervazifeh, A.; Nikbakht, A.M.; Moghaddam, P.A.; Sharifian, F. Energy economy and kinetic investigation of sugar cube dehydration using microwave supplemented with thermal imaging. *J. Food Process. Preserv.* **2018**, *42*, e13504. [CrossRef]
49. Ozgener, L.; Ozgener, O. Exergy analysis of industrial pasta drying process. *Int. J. Energy Res.* **2006**, *30*, 1323–1335. [CrossRef]
50. Zalazar-Garcia, D.; Roman, M.C.; Fernandez, A.; Asensio, D.; Zhang, X.; Fabani, M.P.; Rodriguez, R.; Mazza, G. Exergy, energy, and sustainability assessments applied to RSM optimization of integrated convective air-drying with pretreatments to improve the nutritional quality of pumpkin seeds. *Sustain. Energy Technol. Assess.* **2022**, *49*, 101763. [CrossRef]
51. Zohrabi, S.; Seiiedlou, S.S.; Aghbashlo, M.; Scaar, H.; Mellmann, J. Enhancing the exergetic performance of a pilot-scale convective dryer by exhaust air recirculation. *Drying Technol.* **2019**, *38*, 518–533. [CrossRef]
52. Onwude, D.I.; Hashim, N.; Abdan, K.; Janius, R.; Chen, G. Investigating the influence of novel drying methods on sweet potato (Ipomoea batatas L.): Kinetics, energy consumption, color, and microstructure. *J. Food Process. Eng.* **2018**, *41*, e12686. [CrossRef]
53. Rostami Gharkhloo, Z.; Sharifian, F.; Rahimi, A.; AkhoundzadehYamchi, A. Influence of high wave sound pretreatment on drying quality parameters of Echinacea root with infrared drying. *J. Sci. Food Agr.* **2022**, *102*, 2153–2164. [CrossRef] [PubMed]
54. Harish, A.; Rashmi, M.; Krishna Murthy, T.P.; Blessy, B.M.; Ananda, S. Mathematical modeling of thin layer microwave drying kinetics of elephant foot yam (Amorphophallus paeoniifolius). *Int. Food Res. J.* **2014**, *21*, 1081–1087.
55. Bassey, E.J.; Cheng, J.-H.; Sun, D.-W. Thermoultrasound and microwave-assisted freeze-thaw pretreatments for improving infrared drying and quality characteristics of red dragon fruit slices. *Ultrasonics Sonochem.* **2022**, *91*, 106225. [CrossRef]
56. Geng, Z.; Torki, M.; Kaveh, M.; Beigi, M.; Yang, X. Characteristics and multi-objective optimization of carrot dehydration in a hybrid infrared /hot air dryer. *LWT* **2022**, *172*, 114229. [CrossRef]
57. Chikpah, S.K.; Korese, J.K.; Sturm, B.; Hensel, O. Colour change kinetics of pumpkin (Cucurbita moschata) slices during convective air drying and bioactive compounds of the dried products. *J. Agr. Food Res.* **2022**, *10*, 100409. [CrossRef]
58. Hadjout-Krimat, L.; Belbahi, A.; Dahmoune, F.; Hentabli, M.; Boudria, A.; Achat, S.; Remini, H.; Oukhmanou-Bensidhoum, S.; Spigno, G.; Madani, K. Study of microwave and convective drying kinetics of pea pods (*Pisum sativum* L.): A new modeling approach using support vector regression methods optimized by dragonfly algorithm techniques. *J. Food Process. Eng.* **2022**, *46*, e14232. [CrossRef]
59. Çetin, N. Prediction of moisture ratio and drying rate of orange slicesusing machine learning approaches. *J. Food Process. Preserv.* **2022**, *46*, e17011. [CrossRef]
60. Beigi, M.; Torki, M.; Khoshnam, F.; Tohidi, M. Thermodynamic and environmental analyses for paddy drying in a semi-industrial dryer. *J. Therm. Anal. Calorim.* **2021**, *146*, 393–401. [CrossRef]
61. Okunola, A.; Adekanye, T.; Idahosa, E. Energy and exergy analyses of okra drying process in a forced convection cabinet dryer. *Res.Agr. Eng.* **2021**, *67*, 8–16. [CrossRef]
62. Beigi, M.; Harchegani, H.B.; Torki, M.; Kaveh, M.; Szymanek, M.; Khalife, E.; Dziwulska-Hunek, A. Experimental and numerical analysis of thermodynamic performance of microwave dryer of onion. *J. Food Process. Eng.* **2022**, *45*, e14116. [CrossRef]
63. Colak, N.; Hepbasli, A. Performance analysis of drying of green olive in a tray dryer. *J. Food Eng.* **2007**, *80*, 1188–1193. [CrossRef]